Kerr-lens mode-locking of an Yb:SALLO laser generating 25 fs pulses at 1090 nm

Zhang-Lang Lin,[1] Huang-Jun Zeng,[1] Zhongben Pan,[2, a)] Pavel Loiko,[3] Valentin Petrov,[4] Xavier Mateos,[5] Ge Zhang,[1] and Weidong Chen[1, 4, a)]

[1]*Fujian Institute of Research on the Structure of Matter, Chinese Academy of Sciences, Fuzhou, 350002 Fujian, China*

[2]*School of Information Science and Engineering, Shandong University, 266237 Qingdao, China*

[3]*Centre de Recherche sur les Ions, les Matériaux et la Photonique (CIMAP), UMR 6252 CEA-CNRS-ENSICAEN, Université de Caen, 6 Boulevard Maréchal Juin, 14050 Caen Cedex 4, France*

[4]*Max Born Institute for Nonlinear Optics and Short Pulse Spectroscopy, Max-Born-Str. 2a, 12489 Berlin, Germany*

[5]*Universitat Rovira i Virgili (URV), Física i Cristal·lografia de Materials (FiCMA), 43007 Tarragona, Spain*

a) *Author to whom correspondence should be addressed: zhongbenpan@sdu.edu.cn and chenweidong@fjirsm.ac.cn*

Abstract: We report on the generation of sub-30 fs pulses from a Kerr-lens mode-locked ytterbium solid-state laser based on a disordered Yb:$SrLaAlO_4$ (Yb:SALLO) crystal as a gain medium. The Yb:SALLO laser, pumped by a spatially single-mode Yb-fiber laser at 979 nm, produces soliton pulses as short as 25 fs at 1090 nm, with average output power of 149 mW at a pulse repetition rate of ~80.7 MHz. The power scaling potential of the Kerr-lens mode-locked laser is exploited by achieving watt-level (1.54 W) average output power at 1081 nm for a somewhat longer pulse duration of 31 fs. This result corresponds to an impressive laser efficiency of 49.7% and a peak power of 468 kW.

Mode-locked (ML) solid-state ytterbium (Yb) lasers, emitting ultrashort pulses with durations of a few optical cycles in the spectral range around 1 μm and operating at high repetition rates (~100 MHz), open up new opportunities for various applications including nonlinear microscopy [1], time-domain spectroscopy [2], and the development of compact broadband THz devices for spectroscopy or imaging [3].

Among the passive mode-locking techniques, Kerr-lens mode locking (KLM) stands out as one of the most promising methods for generation of extremely short laser pulses from solid-state lasers down to a few femtoseconds. Using a structurally ordered laser crystal as a gain medium for generating sub-30 fs

pulses, a KLM thin-disk Yb:YAG laser operating in the strongly self-phase modulation broadened regime produced 27 fs pulses at 1028 nm with an average output power of 3.3 W at a pump power of 315 W [6]. Subsequently, slightly shorter (24-fs) pulses were achieved from a KLM Yb:YAP laser at 1085 nm with an average output power of 186 mW at 87.5 MHz [7]. In the realm of disordered Yb^{3+}-doped laser crystals, sub-30 fs pulses were exclusively generated by KLM lasers based on Yb^{3+}-doped tetragonal calcium aluminates, specifically Yb:$CaGdAlO_4$ (Yb:CALGO) and Yb:$CaYAlO_4$ (Yb:CALYO). Relying on the stimulated Raman scattering assisting spectral broadening, a diode-pumped KLM Yb:CALGO laser generated 22 fs pulses at 1.018 GHz with an average output power only 3 mW [8]. Pumping with a high-brightness Yb-fiber laser at 976 nm, a KLM Yb:CALGO laser delivered pulses as shot as 22 fs at 1040.7 nm with an average output power of 729 mW [9]. Notably, sub-20 fs pulses were directly achieved from a KLM Yb:CALGO laser (17.8 fs at an output power of 26 mW [10]) and a KLM Yb:CALYO one (17 fs at 18 mW [11]), albeit at a modest average output power.

Ytterbium (Yb^{3+}) doped strontium lanthanum aluminate, known as Yb:$SrLaAlO_4$ (abbreviated as Yb:SALLO), belongs to the same family of tetragonal $ABCO_4$-type crystals (sp. gr. *I*4/*mmm*), where A = Ca or Sr, B = Y, La or Gd, and C = Al or Ga. In contrast to Yb:CALGO and Yb:CALYO, Yb:SALLO exhibits a lower melting point and somewhat broader gain profiles [12]. The structure disorder of the SALLO crystal stems from the random distribution of Sr^{2+} and La^{3+} cations over the same lattice sites with C_{4v} symmetry. This random cation distribution induces a variation in the local crystal field around the Yb^{3+} dopant ions, leading to significant inhomogeneous spectral line broadening. As a result, Yb:SALLO displays a "glassy-like" spectroscopic behavior, featuring broadband absorption around the Yb^{3+} zero-phonon line at ~980 nm and presenting flat, smooth, and broad gain profiles extending beyond 1 μm. Despite its disordered structure, Yb:SALLO possesses relatively high thermal conductivity at room temperature (6.06 and 4.30 W/mK along ***a***- and ***c***-axes [12] for 1.18 at.% Yb^{3+} doping). The above

spectroscopic and thermal characteristics of Yb:SALLO make it favorable for development of high-power ultrafast (sub-50 fs) passively ML lasers.

A ML Yb:SALLO laser employing a SEmiconductor Saturable Absorber Mirror (SESAM) delivered 38 fs pulses at a central wavelength of 1071 nm, with an average output power of 86 mW at 59.4 MHz [13]. These pulses were shorter than those observed in the initial demonstration of KLM with this crystal [14]. The nonlinear refractive index n_2 of the Yb:SALLO, calculated using the model of Boling, Glass, and Owyoung [15] with the isostructural Yb:CALGO crystal ($n_2 = 4.1 \times 10^{-13}$ esu at 1 μm [16]) as a reference, amounted to $n_2 = 11.4 \times 10^{-13}$ esu at 1 μm (a polarization-averaged value). The relatively high nonlinear refractive index of Yb:SALLO is in line with the high linear refractive indices of this compound ($n_o = 1.938$ and $n_e = 1.960$ at ~1 μm, calculated from [17]) and agrees with the previous studies for Sr-containing complex oxides. Based on this important prerequisite, in the present work, we explore the potential of the disordered Yb:SALLO crystal for the generation of ultimate pulses via the soft-aperture KLM.

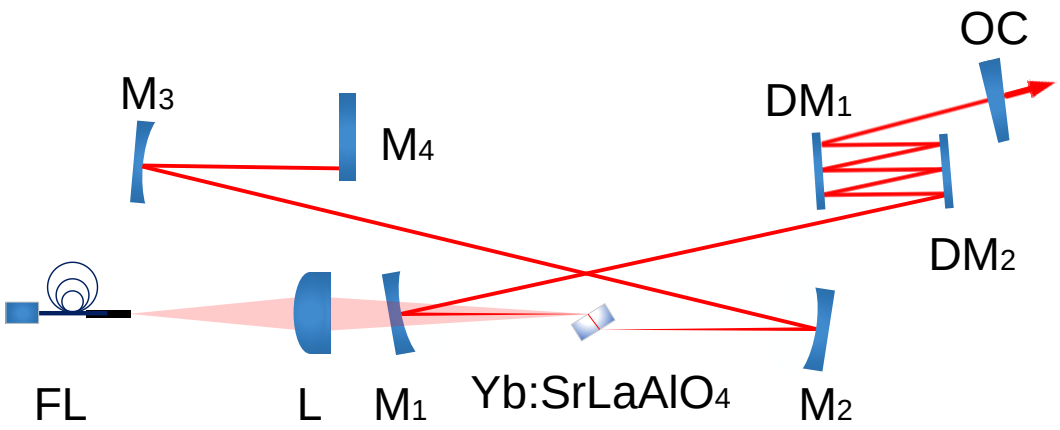

Fig. 1. Schematic of the KLM Yb:SALLO laser setup. FL: Yb fiber laser; L: spherical lens (f = 75 mm); M_1 – M_3, dichroic concave mirrors; M_4: flat rear mirror; DM_1 and DM_2: dispersive mirrors; OC: output coupler.

Figure 1 depicts the schematic of the KLM Yb:SALLO laser set-up. It is based on an asymmetric X-shaped standing-wave cavity with astigmatic compensation. The gain medium is an ***a***-cut Yb:SALLO crystal with an actual Yb^{3+} doping level of 1.18 at.% (ion density: $N_{Yb} = 1.36 \times 10^{20}$ cm^{-3}). The laser

element has dimensions of 3 mm × 3 mm in aperture and is 3 mm-thick. It is mounted in a water-cooled copper holder with a coolant temperature of 20°C and positioned at Brewster's angle between two dichroic concave folding mirrors, M_1 and M_2, both having a radius of curvature (RoC) of -100 mm. The orientation (cut) of the laser crystal is chosen to facilitate access to the desirable π-polarization, thereby enhancing the pump absorption at 979 nm [12] The pump source was a continuous-wave (CW) Yb-fiber laser emitting linearly polarized radiation at 979 nm and featuring a laser linewidth of ~0.1 nm (measured at half maximum, FWHM). The Yb-fiber laser exhibited a nearly diffraction-limited spatial intensity distribution, characterized by a measured beam propagation factor (M_2) of ~1.04. Employing a spherical lens with a focal length of 75 mm, the pump beam was focused into the laser crystal through the M_1 dichroic mirror, resulting in a beam waist (radius) of 15.4 μm × 33 μm in the sagittal and tangential planes, respectively. In one of the cavity arms, an additional concave mirror (M_3, RoC = -100 mm) and a flat rear mirror (M_4) were incorporated. The other arm featured two flat dispersive mirrors (DMs, $DM_1 = DM_2 = -100$ fs^2) and was terminated by a plane-wedged output coupler (OC). The group velocity dispersion (GVD) of the Yb:SALLO crystal was estimated from dispersion curves [18] to be 220 ± 50 fs^2/mm at 1.05 μm for π-polarization.

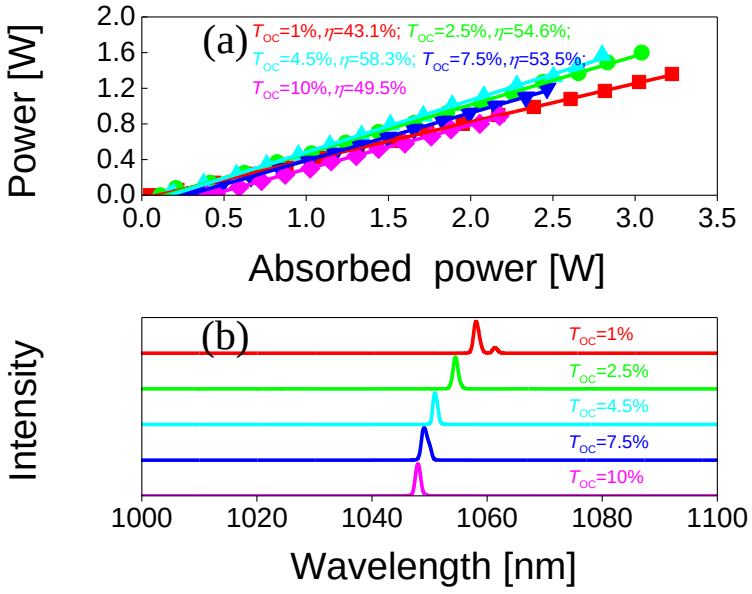

Fig. 2 CW Yb:SALLO laser pumped by an Yb-fiber laser at 979 nm: (a) input – output dependences for different OCs, η – slope efficiency; (b) laser emission spectra measured well above the laser threshold, laser polarization: π.

The Yb:SALLO laser is initially characterized in the CW regime using a set of OCs with a transmission at the laser wavelength (T_{OC}) ranging from 1% to 10%, as illustrated in Fig. 2(a). The measured single-pass pump absorption under lasing conditions decreased with the output coupling in the range of 48.0% - 28.3% due to progressively increasing ground-state bleaching associated with higher population inversion in the laser crystal required to compensate for higher output-coupling losses. For an absorbed pump power of 3 W, a maximum output power of 1.58 W is achieved at 1054.6 nm for an output coupling of 2.5%. This corresponds to a slope efficiency of 54.6% and an optical efficiency of 52.7%. The laser threshold gradually increased with the output coupling, rising from 50 mW (T_{OC} = 1%) to 398 mW (T_{OC} = 10%). The laser wavelength experienced a consistent blue-shift with the increase of the output coupling, in the range of 1058.1 – 1047.9 nm, see Fig. 2(b). This behavior is caused by decreasing reabsorption at higher inversion rates in the gain medium and is typical for quasi-three-level Yb^{3+} lasers.

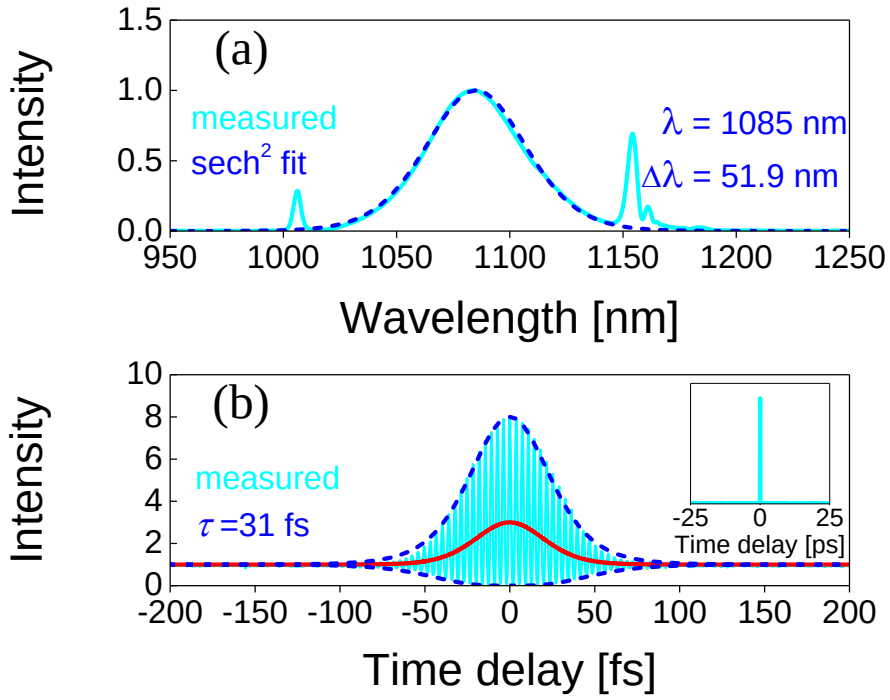

Fig. 3 KLM Yb:SALLO laser with T_{OC} = 2.5%: (a) optical spectrum and (b) interferometric autocorrelation trace. *Inset* in (b): simultaneously measured long-scale (50 ps) autocorrelation trace. The *red curve* in (b) corresponds to the intensity autocorrelation profile.

The DMs were implemented to introduce a round-trip group delay dispersion (GDD) of -1200 fs^2. The KLM operation of the Yb:SALLO laser was first investigated using an intermediate output coupling of 2.5% at an absorbed pump power of 2.0 W. To enhance the self-amplitude modulation (SAM) effect through the soft-aperture KLM, the laser resonator was aligned towards the edge of its stability region by displacing the folding mirror M_2 by several hundred micrometers away from the laser crystal. At this point, the CW output power dropped from about 1 W to 325 mW. The KLM operation was not self-starting, and it required a slight perturbation by gently knocking the OC or adjusting the position of the flat rear mirror M_4. Transition to ML operation of the Yb:SALLO laser was accompanied by a sudden increase in the average output power up to 402 mW. The optical spectrum of the laser pulses is depicted in Fig. 3(a), indicating an emission bandwidth (FWHM) of 51.9 nm at a central wavelength of 1085 nm, assuming a $sech^2$-shaped spectral profile. The recorded interferometric autocorrelation trace shown in Fig. 3(b) gives in a deconvolved pulse duration of 31 fs (FWHM), assuming a $sech^2$-shaped temporal profile. The corresponding time-bandwidth product (TBP) of 0.410 suggests that the pulses are chirped. A long-scale, background-free intensity autocorrelation. scan (50 ps) confirmed single-pulse steady-state mode-locking, as depicted in the inset of Fig. 3(b). This configuration corresponds to a laser efficiency of 20.1% and a peak power of 141 kW.

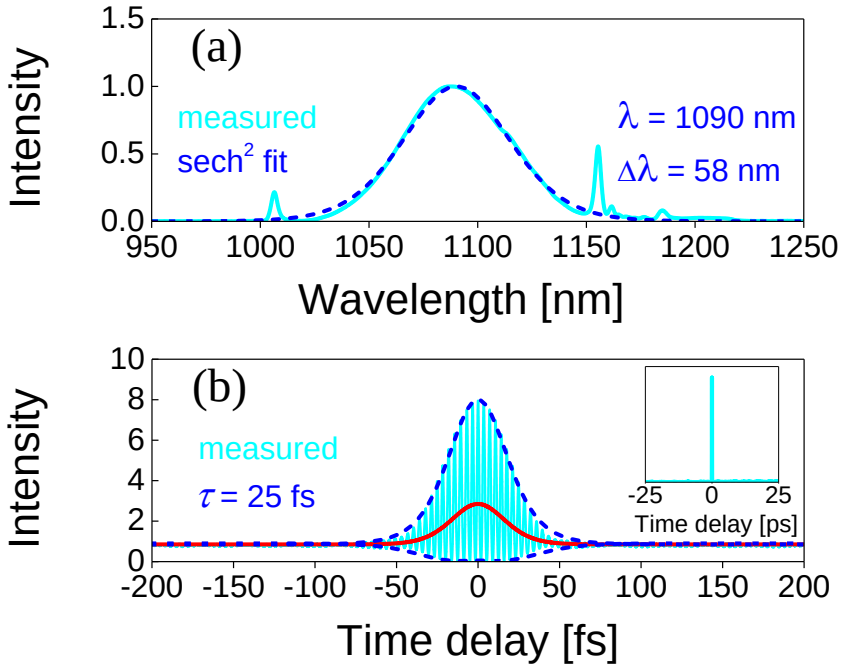

Fig. 4 KLM Yb:SALLO laser with T_{OC} = 0.8%: (a) optical spectrum and (b) interferometric autocorrelation trace. *Inset* in (b): simultaneously measured long-scale (50 ps) autocorrelation trace. The *red curve* in (b) corresponds to the intensity autocorrelation profile.

The pulse duration can be further reduced by reducing the transmittance of the OC. Optimal stability and shortest pulses were obtained with an output coupling of 0.8%, maintaining the same overall negative GDD. The detailed characterization of the laser pulses is outlined in Fig. 4. The laser spectrum, as depicted in Fig. 4(a), is centered at 1090 nm with a spectral bandwidth of 58 nm assuming a sech^2-shaped spectral profile. The pulse duration, estimated from the interferometric autocorrelation trace which is well-fitted with a sech^2-shaped temporal profile as shown in Fig. 4(b), is 25 fs (approximately 7 optical cycles). The corresponding TBP is 0.366, only slightly exceeding the Fourier-transform-limit. The inset in Fig. 4(b) shows the background-free intensity autocorrelation trace over a long-time span of 50 ps, affirming the single-pulse CW-ML operation without any multiple pulse instabilities. The average output power for this OC reached 149 mW at an absorbed pump power of 1.26 W, corresponding to an optical efficiency of 11.8% and a peak power of 65 kW. The KLM laser showed in general no degradation in its output power and its long-term stability was superior compared to SESAM mode-locking with longer pulse durations.

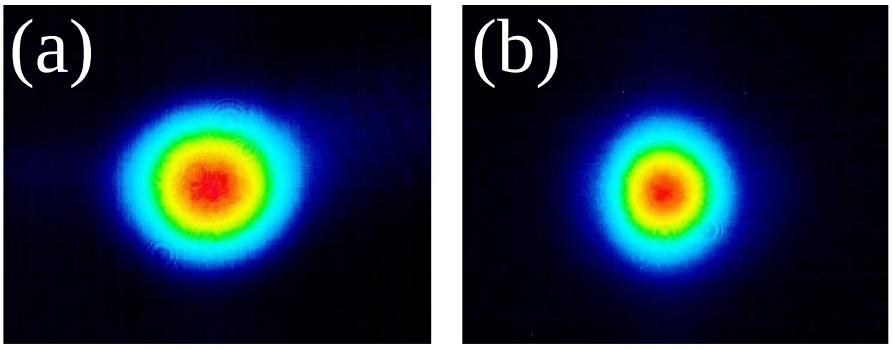

Fig. 5. Measured far-field beam profiles of the Yb:SALLO laser: (a) CW and (b) KLM regimes corresponding to the shortest pulses. T_{OC} = 0.8%.

The high peak intensity of the laser beam inside the laser crystal is expected to cause significant changes in the spatial intensity distribution. This was confirmed by monitoring the far-field beam profiles using a CCD-camera positioned approximately 0.7 m away from the OC. The results showed a reduction in the far-field beam diameter from 2.54×2.06 mm^2 to 2.02×2.05 mm^2, as shown in Fig. 5(a) and (b). This reduction indicates the presence of a strong soft-aperture Kerr-lens effect and self-focusing inside the laser crystal.

Figure 6 illustrates the recorded radio-frequency (RF) spectrum of the steady-state pulse train corresponding to the shortest pulses. In Fig. 6(a), the recorded narrow-band fundamental beat note demonstrates an extremely high extinction ratio of 81 dBc above the carrier at 80.72 MHz. This is an indication of highly stable KLM operation without any Q-switching instabilities or multi-pulsing. Figure 6(b) further confirms the stability by showing uniform harmonic beat notes over a 1-GHz frequency range.

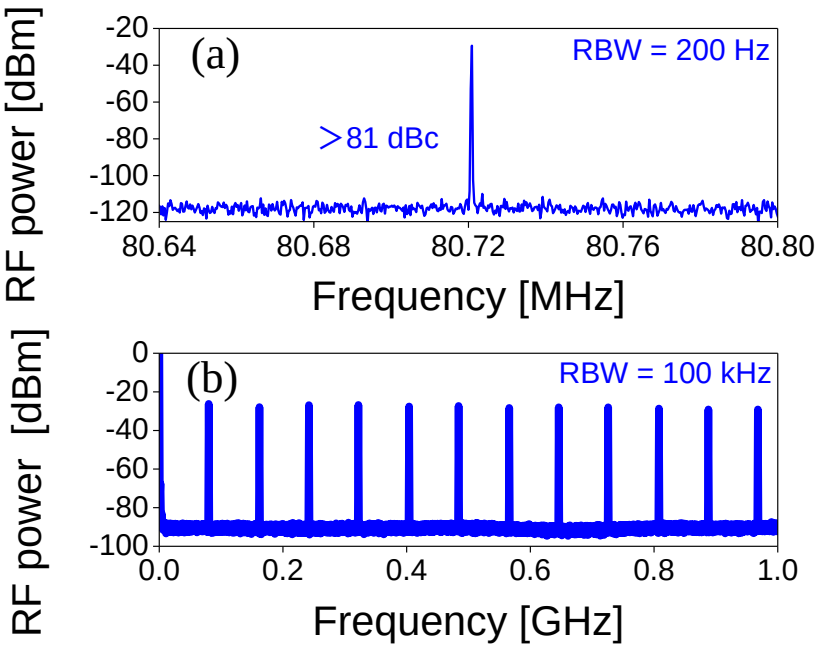

Fig. 6. RF spectra of the KLM Yb:SALLO laser: (a) fundamental beat note, RBW = 200 Hz; (b) 1-GHz span with RBW of 100 kHz. RBW: resolution bandwidth.

The power scalability of the KLM Yb:SALLO laser was investigated by increasing the output coupling to 4%. By adjusting the pump power, single-pulse CW-ML operation was achieved with the highest average output power and laser efficiency. The results, summarized in Table 1, show that the average output power of the KLM Yb:SALLO laser could be scaled up to the watt-level by increasing the output-coupling and the pump power, at somewhat longer pulse duration. The maximum average output power obtained was 1.54 W at an absorbed pump power of 3.1 W, with a pulse duration of 34 fs and a laser efficiency of 49.7%. The spectrum of the KLM laser experienced a slight blue-shift to 1081 nm with 4% output coupling, as expected for the quasi-three-level Yb laser scheme with reabsorption.

Table. 1 Characteristics[a] of the KLM Yb:SALLO Laser vs. Output Coupling

T_{OC} [%]	$\Delta\tau$ [fs]	λ_c [nm]	$\Delta\lambda$ [nm]	P_{out} [W]	P_{abs} [W]	η_{opt} [%]	TBP
0.8	25	1090	58	0.149	1.26	11.8	0.366
1.6	29	1083	56.5	0.223	0.77	28.9	0.419
2.5	31	1085	51.9	0.402	2	20.1	0.410
4%	34	1081	45	1.54	3.1	49.7%	0.393

[a] T_{OC} – output coupler transmittance, $\Delta\tau$ – pulse duration (FWHM), λ_c – central laser wavelength, $\Delta\lambda$ – spectral bandwidth (FWHM), P_{out} – average output power, P_{abs} – absorbed pump power, η_{opt} – optical efficiency referring to absorbed pump power, TBP – time-bandwidth product.

To conclude, Yb:SALLO is a promising material for generating sub-30 fs pulses in Kerr-lens mode-locked lasers due to its broadband emission / gain and relatively high Kerr nonlinearity. In this work, soliton pulses as short as 25 fs were generated at 1090 nm, with an average output power of 149 mW and a pulse repetition rate of 80.72 MHz. These results demonstrate that the exceptionally broad emission bandwidth of Yb:SALLO has the potential to generate sub-50 fs pulses with an average output power potentially reaching tens of Watts using distributed Kerr media and pumping with a high-power, multi-transverse-mode, fiber-coupled InGaAs diode lasers at ~980 nm. Further pulse shortening may be achieved by optimizing the Yb3+ doping concentration as well as using special designed pump mirror so as to fully exploit the gain bandwidth of the Yb:SALLO crystal.

ACKNOWLEDGMENT

National Natural Science Foundation of China (61975208, U21A20508,); Sino-German Scientist Cooperation and Exchange Mobility Program (M-0040); Project of Science and Technology of Fujian Province (2023H0047); Xavier Mateos acknowledges the Serra Húnter program.

AUTHOR DECLARATIONS

The authors declare no conflicts of interest.

Aurthor Contributions

Zhang-Lang Lin: Investigate (lead); Huang-Jun Zeng: Methodology (equal); Zhongben Pan: Resources (lead); Pavel Loiko: Formal analysis (equal); Writing-review & editing (equal); Valentin Petrov: Project administration (equal); Validation (lead); Writing – review & editing (equal); Xavier Mateos: Formal analysis (equal); Writing – review & editing (equal); Ge Zhang: Funding acquisition (equal); Weidong Chen: Conceptualization (lead); Funding acquisition (equal); Projection administration (equal); Supervision (lead); Writing – original draft (lead).

DATA AVAILABILITY

Data underlying the results presented in this paper are not publicly available at this time but may be obtained from the authors upon reasonable request.

References

[1] B. Resan, R. A. Espinosa, S. Kurmulis, J. L. Rodriguez, F. Brunner, A. Rohrbacher, D. Artigas, P. L. Alvarez, and K. J. Weingarten, Opt. Express **22**, 16456 (2014).

[2] G. Cerullo, C. Manzoni, L. Lüer, and D. Polli, Photochem. Photobiol. Sci. **6**, 135 (2007).

[3] J. Takayanagi, H. Jinno, S. Ichino, K. Suizu, M. Yamashita, T. Ouchi, S. Kasai, H. Ohtake, H. Uchida, and N. Nishizawa, Opt. Express **17**, 7533 (2009).

[4] U. Morgner, F. X. Kartner, S. H. Cho, Y. Chen, H. A. Haus, J. G. Fujimoto, E. P. Ippen, V. Scheuer, G. Angelow, and T. Tschudi, Opt. Lett. **24**, 411 (1999).

[5] D. H. Sutter, G. Steinmeyer, L. Gallmann, N. Matuschek, F. Morier-Genoud, U. Keller, V. Scheuer, G. Angelow, and T. Tschudi, Opt. Lett. **24**, 631 (1999).

[6] J. Drs, J. Fischer, N. Modsching, F. Labaye, V. J. Wittwer, and T. Südmeyer, Opt. Express **29**, 35929 (2021).

[7] W. Chen, Z. L. Lin, W. Z. Xue, H. J. Zeng, G. Zhang, P. Loiko, Y. Zhao, X. Xu, J. Xu, X. Mateos, H. Lin, L. Wang, and V. Petrov, Opt. Lett. **47**, 4728 (2022).

[8] S. Kimura, S. Tani, and Y. Kobayashi, Sci. Rep. **9**, 3738 (2019).

[9] F. Labaye, V. J. Wittwer, M. Hamrouni, N. Modsching, E. Cormier, and T. Südmeyer, Opt. Express **30**, 2528 (2022).

[10] Y. Wang, X. Su, Y. Xie, F. Gao, S. Kumar, Q. Wang, C. Liu, B. Zhang, B. Zhang, and J. He, Opt. Lett. 46, 1892 (2021).

[11] J. Ma, F. Yang, W. Gao, X. Xiaodong, X. Jun, D. Shen, and D. Tang, Opt. Lett. 46, 2328 (2021).

[12] Z. Pan, X. Dai, Y. Lei, H. Cai, J. M. Serres, M. Aguiló, F. Díaz, J. Ma, D. Tang, E. Vilejshikova, U. Griebner, V. Petrov, P. Loiko, and X. Mateos, Crystengcomm. **20**, 3388 (2018).
[13] H. J. Zeng, Z. L. Lin, W. Z. Xue, G. Zhang, Z. Pan, H. Lin, P. Loiko, X. Mateos, V. Petrov, L. Wang, and W. Chen, Opt. Express **29**, 43820 (2021).
[14] Z. L. Lin, H. J. Zeng, G. Zhang, W. Z. Xue, Z. Pan, H. Lin, P. Loiko, H. C. Liang, V. Petrov, X. Mateos, L. Wang, and W. Chen, Opt. Express **29**, 42837 (2021).
[15]. R. Adair, L. L. Chase, and S. A. Payne, Phys. Rev. B. **39**, 3337 (1989).
[16] J. Boudeile, F. Druon, M. Hanna, P. Georges, Y. Zaouter, E. Cormier, J. Petit, P. Goldner, and B. Viana, Opt. Lett. **32**, 1962 (2007).
[17] J. Hora, K. Navrátil, J. Humlicek, and M. Berkowski, Phys. Status Solidi B **195**, 625 (1996).
[18] W. Ryba-Romanowski, S. Gołąb, I. Sokolska, W. Pisarski, G. Dominiak-Dzik, A. Pajączkowska, and M. Berkowski, J. Alloys. Compd. **217**, 263 (1995).